Hydrogen on graphene: Electronic structure, total energy, structural distortions and magnetism from first-principles calculations

D. W. Boukhvalov[*]

Institute for Molecules and Materials, Radboud University of Nijmegen, NL-6525 ED Nijmegen, the Netherlands

M. I. Katsnelson

Institute for Molecules and Materials, Radboud University of Nijmegen, NL-6525 ED Nijmegen, the Netherlands

A. I. Lichtenstein

Institute of Theoretical Physics, University of Hamburg, 20355 Hamburg, Germany

Density-functional calculations of electronic structure, total energy, structural distortions, and magnetism for hydrogenated single-layer, bilayer, and multilayer graphenes are performed. It is found that hydrogen-induced magnetism can survive only at very low concentrations of hydrogen (single-atom regime) whereas hydrogen pairs with optimized structure are usually nonmagnetic. Chemisorption energy as a function of hydrogen concentration is calculated, as well as energy barriers for hydrogen binding and release. The results confirm that graphene can be perspective material for hydrogen storage. Difference between hydrogenation of graphene, nanotubes, and bulk graphite is discussed.

I. INTRODUCTION

The discovery of graphene, the first truly two-dimensional crystal, and its exotic electronic properties (for review, see Refs. [1–3]) initiates a huge growth of interest to carbon materials. Most of activity is focused on electronic transport phenomena in graphene, keeping in mind potential applications for carbon-based electronics. However, chemical physics of graphene is also very interesting, in particular, due to opportunity to use graphene for chemical sensors with extraordinary sensitivity.[4] Another interesting direction of investigations is a possible use of graphene for hydrogen storage. One could expect that two-dimensional systems could be very convenient for this aim.

In general, carbon-based systems are among the most attractive objects for hydrogen storage.[5] Promising storage properties of single-walled carbon nanotubes (SWCNTs) were first reported in Ref. [6]. In the past few years graphene was used as a model system to study the electronic structure and adsorption properties of the SWCNTs.[7,8] After the discovery of real graphene several works appeared theoretically studying the hydrogen adsorption on graphene, as a special material (see, e.g., Refs. [9] and [10]). It is commonly accepted now[7–10] that the chemisorption of single hydrogen atom on graphene leads to appearance of magnetic moments in the system. The magnetic interactions between the hydrogen atoms placed at large distances on graphene have been calculated in Ref. [9]. However, energetics of various hydrogen configurations taking into account carbon sheet relaxation was not studied yet in detail. In earlier works, only a very special structure of hydrogenated graphene, with all hydrogens sitting on the same side, was discussed. Here we will demonstrate that actual energetically favorable structure with hydrogenization of the both sides has quite different properties and, in particular, turns out to be nonmagnetic.

Earlier a similar structure has been discussed for the case of SWCNTs.[11,12] However, in contrast with the SWCNTs in graphene there is no specific potential barrier for hydrogen atoms[12] since both sides of graphene are equally achievable for the adsorption which makes the situation different. Deeper understanding of the case of graphene will be useful also to discuss hydrogen storage capacity of nanotubes[7,8] or nonporous carbon,[13] as well as corresponding experimental results for graphite.[14] The effect of curvature on the hydrogen chemisorption in fullerenes and nanotubes has been considered earlier in Ref. [15].

II. CHEMISORPTION OF SINGLE HYDROGEN ATOM

To model the hydrogen chemisorption we use a periodic supercell of graphene containing 32 carbon atoms per each hydrogen atom, similar to Ref. [7]. To consider hydrogen pairs, we will use supercells with 50 carbon atoms for close pairs (neighboring positions of hydrogen) and 72 carbon atoms, otherwise. The density-functional theory calculations were performed using the SIESTA code[16,17] which was successfully applied before to describe hydrogen on graphene.[9] We used the same technical parameters of the calculation as in Ref. [9].

To discuss chemisorption on graphene it is worth to remind its basic electronic structure. Originally, carbon has two $2s$ and two $2p$ electrons. These four electrons produce different kinds of sp-hybridized orbitals.[18] In graphene every carbon atom is bounded with three other carbon atoms via sp^2 hybridization. There are three σ orbitals placed in the graphene plane with angle 120° and one π orbital along Z axis in perpendicular direction. Figure [1] shows the band structure of pure graphene, with three σ bands lying about 3 eV above and below the Fermi level, and π band. In diamond, all carbon atoms are connected via sp^3 hybridization with four σ bands separated by a big gap. Breaking π bonds and producing additional σ bond and, thus, transition from sp^2 to sp^3 hybridization is the main mechanism of chemi-
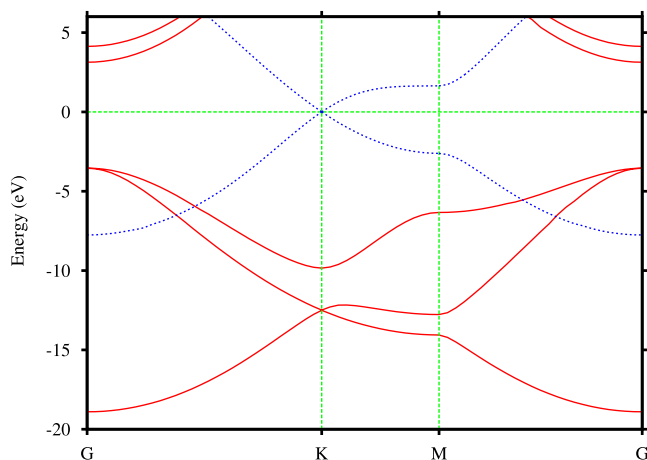
FIG. 1. (Color online) Band structure of a single graphene layer. Solid red lines are σ bands and dotted blue lines are π bands.

sorption on graphene. The crystallographic structure of graphene with two sublattices is shown in Fig. 2. In pure graphene the sublattices are equivalent, but if we bind one of carbon atoms (for example, A_0 in Fig. 2) with hydrogen we automatically break this equivalence.

To check the computational procedure, we reproduce first known results[7–10] for single hydrogen atom chemisorbed on graphene. In agreement with the previous calculations we have found hydrogen-carbon distance about 1.1 Å, and shift of the carbon atom bonded with the hydrogen one about 0.3 Å along Z direction. One should stress, additionally to the previous results, that the atomic distortions are not negligible also for the second and third neighbors of the hydrogen-bonded carbon atom A_0 [see Fig. 3(a)]. The amplitude of the modulation of graphene sheet in the perpendicular direction around the hydrogen atom was estimated as 0.4 Å, which is comparable with the height of intrinsic ripples on graphene of order of 0.7 Å found in atomistic simulations.[19] The radius of the distorted region around hydrogen atom turned out to be about 3.8 Å.

Transformation of the sp^2 hybridization of carbon in ideal graphene to the sp^3 hybridization in hydrogenated graphene results in a change of the bond lengths and angles. A typical
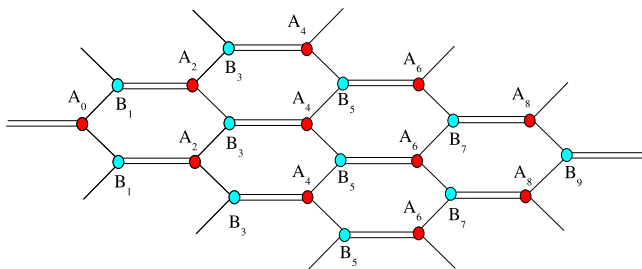

FIG. 2. (Color online) Crystallographic structure of graphene. Red and blue circles show A and B sublattices, respectively. Labels show the distance from A_0 carbon atom (coordination sphere numbers). All bonds in graphene are equivalent, and the double bonds are marked for convenience of comparison with other pictures.
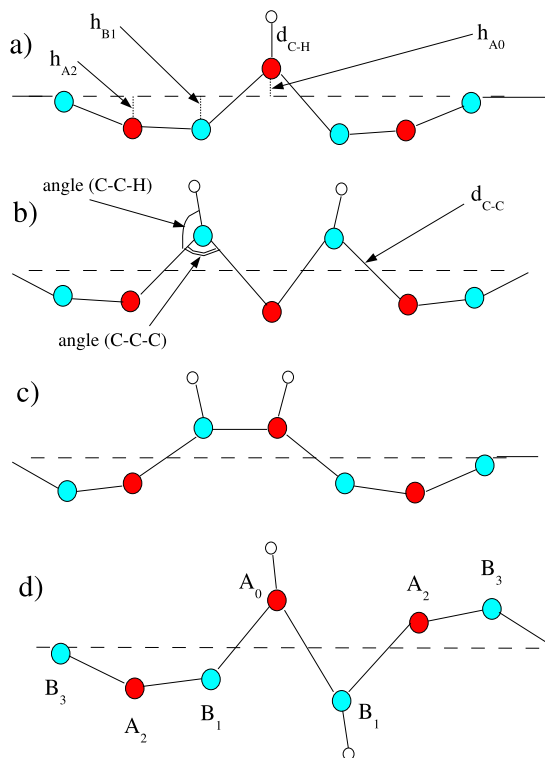

FIG. 3. (Color online) Picture of local distortions of graphene at chemisorption of (a) single hydrogen atom (A_0), (b) two hydrogen atoms bonded with carbon atoms from the same sublattice (A_0-A_2), (c) two hydrogen atoms bonded with neighboring carbon atoms from the same side of graphene sheet (A_0-B_1), and (d) two hydrogen atoms bonded with neighboring carbon atoms from both sides of graphene sheet (A_0-B_1'). Red and blue circles are carbon atoms from two sublattices and white circles are hydrogen atoms.

bond length for sp^2 C—C bonds is 1.42 Å for graphene and graphite and 1.47 Å for other compounds, and the standard bond angle is 120°. For sp^3 hybridization, the standard value of C—C bond length is 1.54 Å, and the angle is 109.5°. A typical value for the single C—H bond length is 1.086 Å. One can see in Table I that for single hydrogen atom the C—H bond length is close to the standard value, but C—C—H and C—C—C angles are intermediate between 90° and 109.5° and 120° and 109.5°, respectively. Also, the length of C—C bond is in between 1.42 and 1.54 Å. This means an intermediate character of the hybridization between sp^2 and sp^3.

A pictorial view of the reconstruction of chemical bonds, with the breaking of double C=C bond and formation of single C—H bond, is shown in Fig. 4. For the case of single hydrogen atom [Fig. 4(a)] this releases two unpaired electrons. One of the electrons forms a bond with hydrogen whereas the other is unpaired. The latter is delocalized in some rather broad area on lattice.[9] As a result, carbon becomes magnetic (see the Table I) and hydrogen atom also possesses a small magnetic moment about $0.12\mu_B$. In general, at the chemisorption of single carbon atom, the hybridization is still rather close to sp^2. One has to consider other opportunities which can lead to sp^3 bonding and possible gain in the chemisorption energy.

TABLE I. Dependence of magnetic moments M (in μ_B), chemisorption energies E_{chem} (in eV), and geometrical parameters (see Fig. 3), in deg. and Å, on configuration of hydrogen (see Fig. 3); d are interatomic distances and h are heights of atoms from graphene plane.

Configuration	M	E_{chem}	h_{A_0}	h_{B_1}	h_{A_2}	Angle (C-C-H)	Angle (C-C-C)	d_{C-H}	d_{C-C}
A_0	1.0	1.441	0.257	−0.047	−0.036	101.3	115.4	1.22	1.496
A_0-A_2	2.0	1.406	0.285	−0.040	−0.096	102.7	116.6	1.132	1.483
A_0-B_1	0.0	0.909	0.364	−0.088	−0.069	102.2	117.5	1.077	1.491
A_0-B_1'	0.0	0.540	0.298	−0.027	−0.035	105.1	106.7	1.112	1.512

III. HYDROGEN PAIRS ON SINGLE-LAYER GRAPHENE

There are four kinds of hydrogen pairs on graphene: hydrogen atoms can be bonded by carbon atoms from the same sublattice from different sublattices, on one side from the graphene sheet, or from both sides. We use the primed indices for the latter case. Computational results for chemisorption of hydrogen pairs are presented in Fig. 3 and Table I. Chemisorption energy per hydrogen atom for the case A_0-A_2 (next-nearest-neighboring carbon atoms, both hydrogen atoms are from the same side) is not significantly different from that for single hydrogen, whereas chemisorption by carbon atoms from different sublattices turns out to be much more energetically favorable.
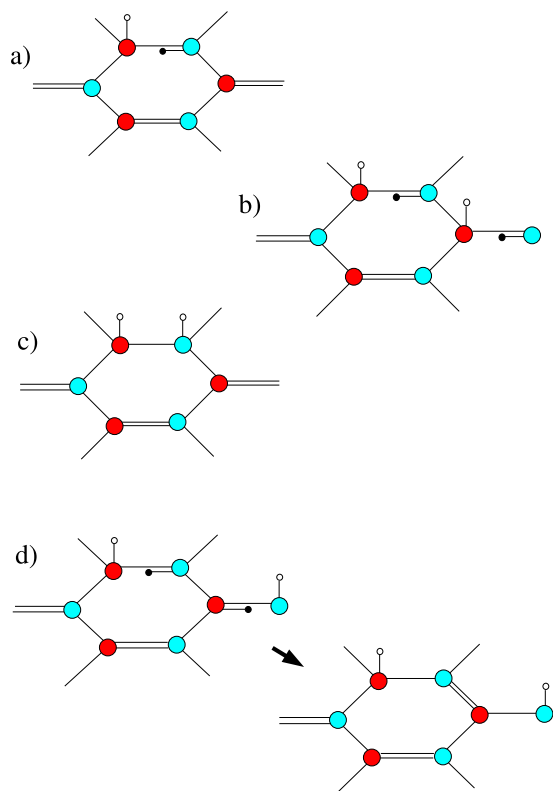
To understand the difference, one has to study what happens with chemical bonds in all these cases. In Fig. 4(b), we can see that for the case A_0-A_2 the situation is basically the same as for the single hydrogen, namely, two broken bonds produce two unpaired electrons with strong ferromagnetic coupling between their spins (dependence of the exchange interactions on interatomic distance was studied in detail in Ref. 9). These electrons in the A_0-A_n case are not paired and produce chemical bonds, the bond distances and angles for A_0-A_2 being intermediate between those typical for the sp^2 and sp^3 hybridization (see Table I).

The situation A_0-B_1 is essentially different. One can see from Fig. 4(c) that, when the double bond between A_0 and B_1 carbon atoms transforms into the single one, two unpaired electrons appear and both of them participate in formation of covalent bonds with the hydrogen atoms. For the case of more distant carbon atoms, say, A_0 and B_3, we can see a similar situation [Fig. 4(d)]. Corresponding changes in the electronic structure for this case are displayed in Fig. 5. The density of states for carbon atoms bonded with hydrogen is redistributed, decreasing in the region between −2.5 and 5 eV (the energy is counted from the Fermi level) and increasing near ±7 eV. These changes correspond to a transition from sp^2 to sp^3 hybridization which makes graphenelike electronic structure more "diamondlike" transforming the π band crossing the Fermi level (see Fig. 1) to fourth σ band

FIG. 4. (Color online) Sketch of chemical bonds for chemisorption of hydrogen: (a) single hydrogen atom (A_0), (b) two hydrogen atoms bonded with carbon atoms from the same sublattice (A_0-A_2), (c) two hydrogen atoms bonded by nearest carbon atoms (A_0-B_1), and (d) two hydrogen atoms bonded by next-nearest carbon atoms from different sublattices (A_0-B_3). Big red (dark) and blue (light) circles are carbon atoms from different sublattices, small white circles are hydrogen atoms, and small black circles are unpaired electrons.
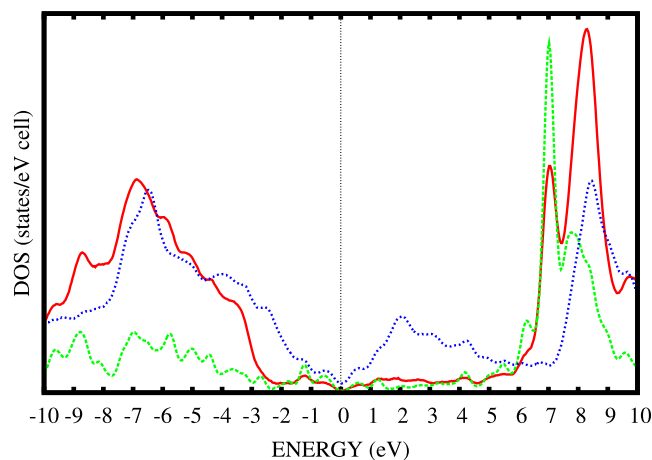

FIG. 5. (Color online) Partial densities of states for carbon atom bound with hydrogen (solid red line), hydrogen atom (dashed green line), and distant carbon atom (from fourth coordination sphere) (dotted blue line) for the case A_0-B_1' configuration [see Fig. 3(d)].
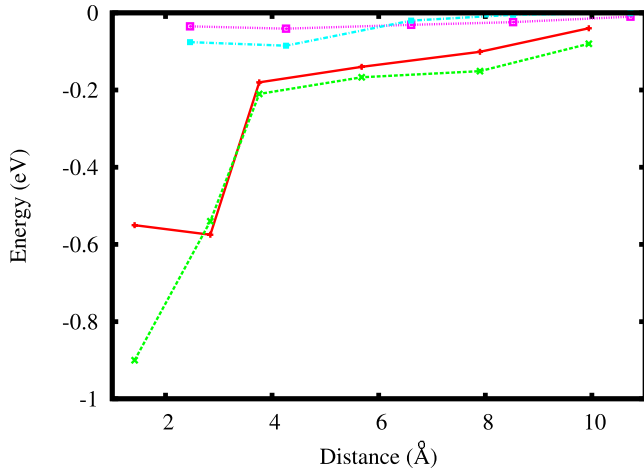
FIG. 6. (Color online) Energy of hydrogen pair (per atom) counted from the energy of single hydrogen atom as a function of interatomic distance: A_0-B_n—solid red line with crosses, A_0-B_n'—dashed green line with crosses, A_0-A_n—dotted light blue line with filled squares, and A_0-A_n'—dot-dashed violet line with empty squares.

lying far from it. At the same time, the electronic structures of fourth neighbors are very close to electronic structure of pure graphene (Fig. 5). In the case of chemisorption by carbon atoms from different sublattices there are no unpaired electrons and no magnetism. In the work[9] this situation was described as antiferromagnetic which is not quite accurate as we believe. Actually, the local magnetic moments just do not survive in this case. The absence of unpaired electrons and broken bonds leads to chemisorption energy gain in comparison with the A-A case described above.

Additionally, we can see in Table I that the C—C bond length for the case A_0-B_1 is close to the standard one for sp^3 hybridization. However, the bond angles are closer to those for sp^2 hybridization, and the chemisorption energy for the case A_0-B_1 is higher than for A_0-B_1'. To understand the difference, one has to investigate structural distortions of graphene sheet. Chemisorption of hydrogen by A_0 carbon atom induces its shift up perpendicular to the plane, together with shifts of atoms B_1 and A_2 in the opposite direction. The chemisorption on carbon B_1 atom shifts B_1 atom up and A_0 and A_2 atoms down. Therefore, for the case A_0-B_1 both A_0 and B_1 carbon atoms move simultaneously in the same direction. As a result, the bond angles become close to those typical for sp^3 hybridization. On the contrary, in A_0-B_1' case the chemisorption of hydrogen from the bottom by B_1 carbon produces shifts up for A_0 and down for B_1 carbon atoms that coincide with the lattice distortion for the bonding of hydrogen by A_0 from the top. In the case A_0-B_1' the lattice distortions produced by chemisorption of each hydrogen atom are consistently working in the same direction providing the lowest chemisorption energy and bond lengths and angles closest to the standard ones for sp^3 hybridization (see Table I).

The calculated dependence of the chemisorption energy on the distance between carbon atoms bonded with hydrogen is presented in Fig. 6. One can see that for all types of pairs the chemisorption energy for the hydrogen atoms closer than

5 Å is lower than for larger distances. Independently of the distance, the nonmagnetic A-B pairs are more energetically favorable than A-A pairs and than noninteracting hydrogen atoms. One can assume therefore that observation of hydrogen-induced ferromagnetism[9] is possible only for a very low concentration of hydrogen when the distance between hydrogen atoms is higher than 12 Å. Our results seem to be in qualitative agreement with the experimental data on hydrogen chemisorption on highly oriented pyrolitic graphite.[20] The pairs A_0-B_3 have been observed which correspond to minimal energy for the one-side hydrogenation of graphene, according to our results (see Fig. 6). Also, at hydrogenation of fullerenes C_{60} the pairs A_0-B_1 and A_0-B_3 (1,2 and 1,4, according to chemical terminology) are usually observed (see, e.g., Ref. 24 and references therein). Instability of magnetic state was observed experimentally for $C_{60}H_{24}$.[25] Recent theoretical results for chemisorption on single[21,22] and multiwalled[23] carbon nanotubes are qualitatively similar to our results for graphene.

IV. HYDROGEN CHEMISORPTION ON BILAYER GRAPHENE

Let us consider now hydrogen chemisorption on graphene bilayer. We studied the chemisorption of single hydrogen atom and pairs of hydrogen atoms placed on one and both sides of the bilayer. The calculations have been performed for two different concentrations of hydrogen, that is, low (32 carbon atoms in each layer per hydrogen atom) and high (8 carbon atoms in each layer per hydrogen atom). Lattice distortions induced by the hydrogen turned out to be different for the case of single-layer and bilayer graphenes. Whereas the shift of carbon atom bound with hydrogen is rather similar in both cases, atomic displacements for the neighboring carbon atoms are much smaller in the case of bilayer. This is not surprising since interlayer coupling tends to make graphene more flat, e.g., sheet corrugations are smaller for suspended bilayer membrane than for the single-layer one.[26]

Computational results are presented in Table II. One can see that for low hydrogen concentration the difference of chemisorption energies between single hydrogen atoms and the pairs is smaller than for the case of singlelayer. There are two configurations which have very close values of the energy for low concentration of hydrogen, A_0-B_1 and A_0-B_3. For the higher concentration, the latter configuration becomes essentially more stable since the lattice distortions are more homogeneous in this case. The effective interactions between hydrogen atoms are more short range in the case of bilayer and already for the configuration A_0-B_5 the chemisorption energy is almost equal to that of two single hydrogen atoms.

In the case of single layer the hydrogen positions on different sides of the graphene sheet are essentially more favorable than those on the same side. Contrary, for the case of bilayer this energy difference is small.

V. HYDROGEN STORAGE PROPERTIES OF GRAPHENE

Chemisorption energy per hydrogen atom for the most favorable case of A_0-B_1' pairs presented in Table I is not very

TABLE II. Chemisorption energy E_{chem} per hydrogen atom (in eV), height h of carbon atom bound with hydrogen up to the layer, and interlayer distance d (in Å) for graphene bilayer for different hydrogen concentrations and configurations of chemisorbed hydrogen.

Concentration	Configuration	E_{chem}	h	d
Low	A_0	1.28	0.639	3.237
	A_0-B_1 one side	0.715	0.570	3.222
	A_0-B_1 both sides	0.713	0.615	3.149
	A_0-B_3 one side	0.720	0.477	3.237
	A_0-B_3 both sides	0.733	0.453	3.237
High	A_0-B_1 one side	0.885	0.445	3.174
	A_0-B_1 both sides	0.850	0.426	3.041
	A_0-B_3 one side	0.381	0.359	3.262
	A_0-B_3 both sides	0.390	0.349	3.198

high. Another limiting case with much higher adsorption energy per hydrogen atom corresponds to the case of fully hydrogenated graphene which is close to a hypothetical compound graphane.[27] For the latter case, we have found bond lengths 1.526 Å for C—C bonds and 1.110 Å for C—H bonds, and bond angles 102.8° and 107.5° for C—C—C and C—C—H angles, respectively, in good agreement with the results of Ref. 27. The calculated values are close to the standard ones for sp^3 hybridization, that is, 1.54 Å for the length of C—C bonds and 109.5° for all angles. Values of C—H bonds are also very close to the standard 1.09 Å.

We studied transition from single pairs to complete coverage changing the supercell size. The dependence of the chemisorption energy on the hydrogen concentration is shown in Fig. 7. For fully hydrogenated graphene the mass percentage of hydrogen (gravimetric energy density) is 7.8 which is over the target value of United States Department of Energy 6.5.[6] Other relevant characteristics for hydrogen storage are energy barriers which are necessary to overcome to start hydrogenation and dehydrogenation. They correspond to the chemisorption energy per hydrogen atom for single hydrogen pair and for fully hydrogenated graphene, respectively. We found for these quantities 0.53 eV (25.5 kJ/mol) and 0.42 eV (20.3 kJ/mol). The latter value is close to the experimental one, 19.6 kJ/mol, for hydrogenized nanotubes.[6] These values look quite reasonable in view of potential applications of graphene for the hydrogen storage. Transformation of electronic structure with increasing hydrogen concentration presented on the insets of Fig. 7. Minimal mass hydrogen concentration which results in opening of energy gap at the Fermi level is about 4.04 (50% coverage), the gap value being 1.75 eV. This seems to be, potentially, an interesting prediction for experiment, although it is not clear whether it is possible to stabilize this configuration or not.

The computational results under discussion have been obtained in the generalized gradient approximation (GGA), which is a common practice for electronic structure calculations of H—C systems.[7–9,28] To estimate possible errors we have calculated the desorption energy in the local density approximation (LDA) as well. We have obtained the value
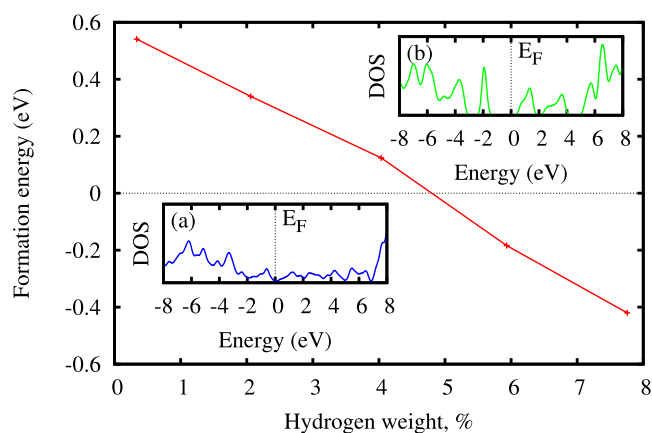

FIG. 7. (Color online) Dependence of the chemisorption energy per hydrogen atom on the mass hydrogen concentration (gravimetric energy density). The inset shows total densities of states for for (a) 2.06 and (b) 4.04 mass hydrogen concentrations.
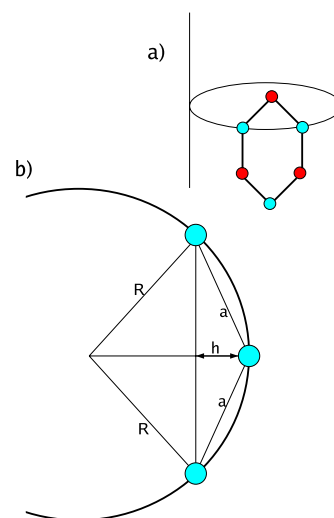

FIG. 8. (Color online) (a) Position of carbon hexagons on surface of SWCNTs. Red (dark) and blue (light) circles are carbon atoms from different sublattices. (b) Position of carbon atoms on radii of SWCNTs.

TABLE III. Dependence of chemisorption energy (in eV), interlayer distance d, and geometrical parameters (in Å) (see Fig. 3) on numbers of graphene layers for 50% hydrogenation of one side of the top layer.

No. of layers	E_{chem}	d	h_A	h_B	d_{C-H}	d_{C-C}
1	1.775		0.106	0.143	1.158	1.475
2	1.452	2.88	0.142	0.198	1.154	1.475
5	1.621	3.124 and 3.353	0.133	0.116	1.164	1.468

0.62 eV, in comparison with the GGA result 0.42 eV so the difference is essential. In more detail, the question was studied in Ref. 28 with the conclusion that GGA is more reliable than LDA for this kind of problems.

In previous works[7,8] hydrogenation of graphene was studied as a model of that of SWCNTs. However, these two situations are not identical due to curvature of the nanotubes. In Fig. 8 we sketch the SWCNTs, value h from Fig. 8(b) corresponding to the sum of the values h_{A_0} and h_{A_2} from Fig. 3(a). In SWCNTs $h = a^2/2R$, where a is the lattice parameter for graphene, 2.46 Å, and R is the radius of nanotube. Typical diameters of the SWCNTs 10–15 Å correspond to the values of h from 0.605 to 0.375 Å. At the same time, single hydrogen atom on graphene produces a distortion with the value $h = 0.293$ Å, which is lower than for the SWCNTs of standard diameter. This value is close to those for theoretical estimations of maximum of the SWCNT diameter, 41.6 and 49.9 Å.[29,30]

On the other hand, multiwalled carbon nanotubes (MWCNTs) have typical diameters about 50 Å and bilayer graphene can be a reasonable model to study hydrogenation of the MWCNTs. Moreover, partial graphitization and presence of metallic catalysts strongly influence on adsorption properties of SWCNTs[6] whereas graphene is perfectly pure material. Other problems for hydrogenation of nanotubes are how to provide an access of hydrogen to their surface in an array[31] and high enough flip into energy barrier.[12] Carbon 1s x-ray photoemission spectra of the SWCNTs before hydrogenation, after hydrogenation, and after dehydrogenation reported in Ref. 32 are all different which could be in part due to defect formation whereas graphene has a very high vacancy formation energy (up to 8 eV) which means much higher stability of graphene under high temperatures and pressures.

At last, we compared hydrogen storage properties of graphene and graphite nanofibers (GNFs), that is, very small graphite platelets, with a size of order of 30–500 Å.[33] Raman spectra for graphene multilayers become very close to ones for graphite when the number of layers is five or more so one can assume that five-layer graphene is already similar to the bulk case.[34] To model the GNFs we used therefore five-layer graphene slab. Complete one-side hydrogenation of GNFs, as well as of graphene, is impossible and only 50% hydrogenation of the top layer is supposed to be the maximum (all carbon atoms from one of the sublattices are bonded with hydrogens) that corresponds to approximately 1% of gravimetric energy density. The calculated chemisorption energy per hydrogen for single-layer graphene with the same gravimetric energy density is 0.32 eV lower than for five-layer graphene. The maximum load of the five-layer graphene is 2% of the gravimetric energy density that is about four times smaller than for the single-layer graphene. Results of calculation for the case of 50% hydrogenated surface of graphene single layer, bilayer, and graphite (five layers of graphene) are presented in Table III. For all three structures chemisorption energies, structural changes, magnetic properties, and electronic structures are essentially different. Some differences, e.g., in the length of C—H bond are negligible, but many others (amplitude of bending distortions) are significant. Detailed comparison of chemical and structural properties of single-layer and multilayer graphenes will be reported elsewhere.

VI. CONCLUSIONS

We have performed the density-functional calculations of electronic structure, magnetic properties, and energetics of different hydrogenated grephene layers. Our results support a suggestion that graphene may be a promising material for the hydrogen storage. Equivalence of two sides of graphene distinguishes it drastically from the nanotubes. We have shown that the most stable configuration of low hydrogenated grephene layer corresponds to the non-magnetic pair hydrogen atoms attached to the different A-B sublattices of graphene from the different sides. It is worth to emphasize that single-layer[13] or bilayer[35,36] graphene should be rather carefully used as models of structural and chemical properties of graphite and its derivates. Also, a comparison of experimental results for graphite[14] with the computational results for graphene sheets[9] requires additional investigation.

ACKNOWLEDGMENTS

*d.bukhvalov@science.ru.nl

[1] A. K. Geim and K. S. Novoselov, Nat. Mater. **6**, 183 (2007).

[2] M. I. Katsnelson, Mater. Today **10**, 20 (2007).

[3] Special issue of Solid State Commun. **143**, 1 (2007), edited by S. Das Sarma, A. K. Geim, P. Kim, and A. H. MacDonald.

[4] F. Schedin, A. K. Geim, S. V. Morozov, E. W. Hill, P. Blake, M. I. Katsnelson, and K. S. Novoselov, Nat. Mater. **6**, 652 (2007).

[5] A. C. Dillon and M. J. Heben, Appl. Phys. A: Mater. Sci. Process. **72**, 133 (2001).

[6] A. C. Dillon, K. M. Jones, T. A. Bekkedahl, C. H. Kiang, D. S. Bethune, and M. J. Heben, Nature (London) **386**, 377 (1997).

[7] P. O. Lehtinen, A. S. Foster, Y. Ma, A. V. Krasheninnikov, and R. M. Nieminen, Phys. Rev. Lett. **93**, 187202 (2004).

[8] E. J. Duplock, M. Scheffler, and P. J. D. Lindan, Phys. Rev. Lett. **92**, 225502 (2004).

[9] O. V. Yazyev and L. Helm, Phys. Rev. B **75**, 125408 (2007).

[10] A. Ito, H. Nakamura, and A. Takayama, arXiv:cond-mat/0703377 (unpublished).

[11] J. Li, T. Furuta, H. Goto, T. Ohashi, Y. Fujiwara, and S. Yip, J. Chem. Phys. **119**, 2376 (2003).

[12] S. M. Lee, K. H. An, Y. H. Lee, G. Seifert, and T. Frauenheim, J. Am. Chem. Soc. **123**, 5059 (2001).

[13] J. M. Carlsson and M. Scheffler, Phys. Rev. Lett. **96**, 046806 (2006).

[14] P. Esquinazi, D. Spemann, R. Höhne, A. Setzer, K.-H. Han, and T. Butz, Phys. Rev. Lett. **91**, 227201 (2003).

[15] P. Ruffieux, O. Gröning, M. Bielmann, P. Mauron, L. Schlapbach, and P. Gröning, Phys. Rev. B **66**, 245416 (2002).

[16] E. Artacho, J. D. Gale, A. Garsia, J. Junquera, R. M. Martin, P. Orejon, D. Sanchez-Portal, and J. M. Soler, SIESTA, Version 1.3, 2004.

[17] J. M. Soler, E. Artacho, J. D. Gale, A. Garsia, J. Junquera, P. Orejon, and D. Sanchez-Portal, J. Phys.: Condens. Matter **14**, 2745 (2002).

[18] L. Pauling, *The Nature of the Chemical Bond* (Cornell University Press, New York, 1960).

[19] A. Fasolino, J. H. Los, and M. I. Katsnelson, Nat. Mater. **6**, 858 (2007).

[20] L. Hornekær, Ž. Šljivančanin, W. Xu, R. Otero, E. Rauls, I. Stensgaard, E. Lægsgaard, B. Hammer, and F. Besenbacher, Phys. Rev. Lett. **96**, 156104 (2006).

[21] G. Buchs, A. V. Krasheninnikov, P. Ruffieux, P. Gröning, A. S. Foster, R. M. Nieminen, and O. Groning, New J. Phys. **9**, 275 (2007).

[22] D. Stojkovic, P. E. Lammert, and V. H. Crespi, Phys. Rev. Lett. **99**, 026802 (2007).

[23] Z. H. Xia, P. R. Guduru, and W. A. Curtin, Phys. Rev. Lett. **98**, 245501 (2007).

[24] M. Prato, J. Mater. Chem. **7**, 1097 (1997).

[25] V. E. Antonov, I. O. Bashkin, S. S. Khasanov, A. P. Moravsky, Yu. G. Morozov, Yu. M. Shulga, Yu. A. Osipyan, and E. G. Ponyatovsky, J. Alloys Compd. **330–332**, 365 (2002).

[26] J. C. Meyer, A. K. Geim, M. I. Katsnelson, K. S. Novoselov, D. Obergfell, S. Roth, C. Girit, and A. Zettl, Solid State Commun. **143**, 101 (2007).

[27] J. O. Sofo, A. S. Chaudhari, and G. D. Barber, Phys. Rev. B **75**, 153401 (2007).

[28] S. M. Lee, K. S. Park, Y. C. Choi, Y. S. Park, J. M. Bok, D. J. Bae, K. S. Nahm, Y. G. Choi, S. C. Yu, N.-g. Kim, T. Frauenheim, and Y. H. Lee, Synth. Met. **113**, 209 (2000).

[29] J. A. Elliott, J. K. W. Sandler, A. H. Windle, R. J. Young, and M. S. P. Shaffer, Phys. Rev. Lett. **92**, 095501 (2004).

[30] T. Tang, A. Jagota, C.-Y. Hui, and N. J. Glassmaker, J. Appl. Phys. **97**, 074310 (2005).

[31] Q. Wang and J. K. Johnson, J. Phys. Chem. B **103**, 4809 (1999).

[32] A. Nikitin, H. Ogasawara, D. Mann, R. Denecke, Z. Zhang, H. Dai, K. Cho, and A. Nilsson, Phys. Rev. Lett. **95**, 225507 (2005).

[33] A. Chambers, C. Park, R. T. K. Baker, and N. M. Rodrigez, J. Phys. Chem. B **102**, 4253 (1998).

[34] A. C. Ferrari, J. C. Meyer, V. Scardaci, C. Casiraghi, M. Lazzeri, F. Mauri, S. Piscanec, D. Jiang, K. S. Novoselov, S. Roth, and A. K. Geim, Phys. Rev. Lett. **97**, 187401 (2006).

[35] Y. Ferro and A. Allouche, Phys. Rev. B **75**, 155438 (2007).

[36] O. V. Yazyev, I. Tavernelli, U. Rothlisberger, and L. Helm, Phys. Rev. B **75**, 115418 (2007).